Journal of Clinical and Translational Pathology **2023** vol. 3(2) | 49–58
DOI: 10.14218/JCTP.2022.00031

Original Article

Androgen Drives the Expression of SARS-CoV-2 Entry Proteins in Sinonasal Tissue

Rong Rong Huang[1*], Jenna M. Giafaglione[2], Takao Hashimoto[2], Liying Zhang[1], Weibo Yu[1], Jianyu Rao[1], Joshua W. Russo[3], Steven P. Balk[3], Nicholas G. Nickols[4,5], Mathew B. Rettig[6,7,8], Andrew Goldstein[2] and Huihui Ye[1,8,9*]

[1]Department of Pathology and Laboratory Medicine, University of California, Los Angeles, CA, USA; [2]Department of Molecular, Cell & Developmental Biology, University of California, Los Angeles, CA, USA; [3]Hematology-Oncology Division, Department of Medicine and Cancer Center, Beth Israel Deaconess Medical Center, Boston, MA, USA; [4]Department of Radiation Oncology, University of California, Los Angeles, CA, USA; [5]Department of Radiation Oncology, VA Greater Los Angeles Healthcare System, Los Angeles, CA, USA; [6]Division of Hematology-Oncology, Department of Medicine, VA Greater Los Angeles Healthcare System, Los Angeles, CA, USA; [7]Department of Medicine, University of California, Los Angeles, CA, USA; [8]Department of Urology, University of California, Los Angeles, CA, USA; [9]Department of Pathology and Laboratory Medicine, Cedars-Sinai Medical Center, Los Angeles, CA, USA

Received: November 29, 2022 | **Revised:** March 3 2023 | **Accepted:** March 8, 2023 | **Published online:** May 1, 2023

Abstract

Background and objectives: Men have higher morbidity and mortality from COVID-19 than women, possibly due to androgen receptor-regulated viral entry protein expression. This led to a clinical trial of androgen deprivation therapy (ADT), which has not shown a significant benefit in the outcomes among hospitalized male COVID-19 patients. The aim of this study was to explore biological explanations for the failure of ADT to mitigate clinical outcomes in men with severe COVID-19 by assessing the role of androgen in regulating viral entry protein expression in the upper and lower respiratory tract. ***Methods:*** Immunohistochemistry was used to assess the expression of transmembrane serine protease 2 (TMPRSS2) and angiotensin-converting enzyme 2 (ACE2) and how it correlated to androgen receptor expression in the sinonasal epithelium, minor salivary glands of the sinus, lacrimal glands, and lungs from mice pretreated with and without castration and ADT as well as the sinonasal epithelium obtained from healthy human donors and hospitalized COVID-19 patients. ***Results:*** In murine models, castration and ADT treatment downregulated the expression of TMPRSS2 and ACE2 in the sinonasal epithelium, minor salivary glands of the sinus, and lacrimal glands, but not in the lungs. Correlative analyses using human tissue also showed a potential role of ADT in men during the early sinonasal phase but not in the later lung phase of SARS-CoV-2 infection. ***Conclusions:*** Our study suggests a potential benefit of ADT in male patients with early COVID-19 when the virus enters the nasopharynx, but not in those with advanced disease. The downregulation of viral entry proteins in the upper respiratory system following androgen blockade may be a key mechanism for this effect.

Citation of this article: Huang RR, Giafaglione JM, Hashimoto T, Zhang L, Yu W, Rao J, *et al*. Androgen Drives the Expression of SARS-CoV-2 Entry Proteins in Sinonasal Tissue. J Clin Transl Pathol 2023;3(2):49–58. doi: 10.14218/JCTP.2022.00031.

Keywords: SARS-CoV-2; COVID-19; Androgen deprivation therapy; Viral entry proteins; Androgen receptor; TMPRSS2; ACE2.

Abbreviations: ACE2, angiotensin-converting enzyme 2; ADT, androgen deprivation therapy; AR, androgen receptor; HITCH, Hormonal Intervention for the Treatment in veterans with COVID-19 requiring Hospitalization; IHC, immunohistochemistry; NP, nasopharyngeal; PCa, prostate cancer; PDX, patient-derived xenograft; PSA, prostate-specific antigen; S, spike; TMPRSS2, transmembrane serine protease 2.

[*]**Correspondence to:** Rong Rong Huang, Department of Pathology and Laboratory Medicine, University of California, Los Angeles, CA 90095, USA. ORCID: https://orcid.org/0000-0001-5308-8024. Tel: +1-310-825-1157, Fax: +1-310-825-2086, E-mail: RHuang@mednet.ucla.edu; Huihui Ye, Department of Pathology and Laboratory Medicine, Cedars-Sinai Medical Center, Los Angeles, CA. ORCID: https://orcid.org/0000-0002-8307-9492. Tel: +1-310-423-1371, Fax: +1-310-248-6233, E-mail: huihui.ye@cshs.org

Introduction

The morbidity and mortality of COVID-19 are higher in men than women, whereas the incidence is only slightly higher in women.[1] The gender disparity indicates a potential role of androgen and/or estrogen in the regulation of viral infection in target cells and in the host immune response. SARS-CoV-2 viral entry into host cells is mediated by the interaction between the viral spike (S) protein and two host cell-surface molecules: receptor angiotensin-converting enzyme 2 (ACE2) and S protein primer transmembrane serine protease 2 (TMPRSS2). TMPRSS2 cleaves the S protein and allows the activated S protein to bind to its receptor ACE2. Furin, another cell-surface protease, is also involved in S protein priming by cleaving the S protein on a second proteolytic site.[2] TMPRSS2 is known to be transcriptionally upregulated by androgen in the human prostate and in prostate cancer (PCa). Approximately 40% of human PCa harbors a translocation between the *TMPRSS2* and *ERG* genes, leading to androgen-dependent overexpression of ERG oncoprotein. In early 2020, a study from Italy showed that PCa patients on androgen dep-

rivation therapy (ADT) had a significantly lower incidence of COVID-19 compared to PCa patients not on ADT.[3]

Based on the above evidence, we hypothesized that ADT may be able to suppress SARS-CoV-2 viral entry into target cells through the downregulation of TMPRSS2 and perhaps ACE2 and furin. Two phase 2 randomized, double-blind, placebo-controlled clinical trials, including our "Hormonal Intervention for the Treatment in veterans with COVID-19 requiring Hospitalization (HITCH)" study (ClinicalTrials.gov Identifier: NCT04397718), failed to demonstrate that rapid suppression of serum androgen levels to a castrate range affected the clinical outcomes of men hospitalized for COVID-19.[4,5] During the trial, several independent studies reported preclinical evidence in animal models and cell lines that androgen deprivation or androgen receptor (AR) antagonists reduce SARS-CoV-2 host cell entry.[6–8] In this study, we aimed to critically evaluate the role of androgen in regulating TMPRSS2, ACE2, and furin protein expression in the upper and lower respiratory tract epithelium.

Methods

Cell lines, xenografts, and patient-derived xenograft (PDX) models

The cell lines used in this study (LNCaP, A549, H441, H2170) were purchased from the American Type Culture Collection (Manassas, VA, USA) and cultured in the recommended media. 16D cells were obtained from Dr. Amina Zoubeidi (Vancouver Prostate Centre, BC, Canada) and maintained as previously described. The cells were grown on plates coated with 0.01% poly-L-lysine (Sigma; St. Louis, MO, USA) to enhance attachment. Enzalutamide (Selleck Chemicals; Houston, TX, USA; 10 μM) or apalutamide (Janssen Research & Development; Titusville, NJ, USA; 10 μM), was replenished every other day for the period specified in each figure. For the castration experiments, the cells were cultured in media supplemented with charcoal-stripped fetal bovine serum (Sigma). LNCaP cells were used for the subcutaneous xenograft injections within four passages. Six-week-old male ICR/scid mice (Taconic Biosciences, Germantown, NY, USA) were injected subcutaneously with 5 million LNCaP cells in 100% Matrigel to generate LNCaP xenografts. The BID-PC-1 PDX was passaged in intact male ICR/scid mice and was hormone-sensitive. Xenograft and PDX tumors were grown until they reached a volume of approximately 1,000 mm^3, and then the mice were castrated, or castrated and placed on enzalutamide (50 mg/kg/day) in drinking water. Seven days following castration or castration+enzalutamide, the mice were euthanized and the tumors were harvested.

Mouse experiments

Male C57BL/6J and C57BL/6N mice (B6) were purchased from Jackson Laboratories (Bar Harbor, ME, USA) and housed under the care and supervision of veterinarians from the Division of Laboratory Animal Medicine at the University of California, Los Angeles (USA). The mice were treated with either 10 mg/kg/day enzalutamide (Selleck Chemicals; S1250) p.o., 50 mg/kg/day bicalutamide (Santa Cruz Biotechnology, Santa Cruz, CA, USA; sc-202976A) i.p., or vehicle. The vehicle used was 1% carboxymethyl cellulose (Sigma; 419273), 0.5% Tween 80 (Fisher Scientific, Waltham, MA, USA; BP338-500), and 5% dimethyl sulfoxide (Fisher Scientific; BP231-100) for enzalutamide, and 100% dimethyl sulfoxide for bicalutamide. Castrated mice were purchased from Jackson Laboratories. The lungs, prostate, and head/nose portions were dissected, fixed in formalin, decalcified using Immunocal (StatLab, McKinney, TX, USA; 1414-32) if containing bones, and prepared for paraffin sections. Half of those organs were lysed with radioimmunoprecipitation assay buffer (Thermo Scientific; 89901) with protease inhibitor (Sigma; CO-RO) and phosphatase inhibitor (Thermo Scientific; 78428) for protein analysis. For the protein extract of the nasal mucosa, the skull was taken off from the posterior part of the body and the mandible. The skin, muscle, and brain were removed from the skull, and the remaining mucosal tissue and bone were submerged in lysis buffer and mixed by vortexing. After 30 min of incubation on ice, the lysis buffer was collected and sonicated. For immunostaining, the tissue was fixed with 4% paraformaldehyde in phosphate-buffered saline (diluted from 16% solution; Electron Microscopy Sciences, Hatfield, PA, USA; 15710) for 6–8 h at room temperature and then processed for paraffin sections. For mouse prostate immunohistochemistry (IHC) following abiraterone and enzalutamide treatment, the ICR/scid male mice were maintained at the animal facility at the Beth Israel Deaconess Medical Center (Boston, MA, USA). The mice were given abiraterone acetate (30 mg/kg/day) or enzalutamide (50 mg/kg/day) in drinking water for 10 days. Following the 10-day treatment, the mice were euthanized. The prostate with attached seminal vesicles was dissected out, fixed with 4% paraformaldehyde in phosphate-buffered saline, and then processed for paraffin sections.

This study was carried out in accordance with the recommendations in the Guide for the Care and Use of Laboratory Animals of the National Institutes of Health. The protocol was approved by the Animal Research Committee on the Ethics of Animal Experiments of the University of California at Los Angeles (Protocol Number: ARC-2017-020). All surgeries were performed under sodium pentobarbital anesthesia, and all efforts were made to minimize suffering.

Western blot and RNA sequencing

Cells were lysed in radioimmunoprecipitation assay buffer (50 mM Tris-HCl pH 8.0, 150 mM NaCl, 1% NP-40, 0.5% sodium deoxycholate, 0.1% sodium dodecyl sulfate; Fisher Scientific) containing a complete protease inhibitor cocktail tablet (Roche, Indianapolis, IN, USA) and Halt Phosphatase Inhibitor (Fisher Scientific). Each sample was sonicated for 40 s at 20 kHz with a sonic dismembrator (Fisher Scientific) to improve the membranous and nuclear protein yield. Samples were run on NuPAGE 4–12% Bis-Tris Gel (Invitrogen, Waltham, MA, USA) and transferred onto 0.45-μm polyvinylidene fluoride membranes (Millipore Sigma, Burlington, MA, USA). Total protein was visualized using SYPRO RUBY protein blot stain (Fisher Scientific), and membranes were blocked in phosphate-buffered saline + 0.1% Tween-20 (Fisher Scientific) + 5% milk (Fisher Scientific) for 1 h. The membranes were probed overnight at 4°C with the following primary antibodies: prostate-specific antigen (PSA; Cell Signaling Technology, Danvers, MA, USA; 5877, 1:1,000), TMPRSS2 (Abcam; Waltham, MA, USA; 92323, 1:1,000), vinculin (Abcam; 129002, 1:6,000), AR (Cell Signaling Technology; 5153, 1:2,000), furin (Abcam; 183495, 1:1,000), glyceraldehyde 3-phosphate dehydrogenase (GeneTex; Irvine, CA, USA; GT239, 1:10,000). The membranes were then incubated with chromophore-conjugated secondary antibodies (Fisher Scientific) or horseradish peroxidase-conjugated secondary antibodies (Fisher Scientific) for 1 h and detected via florescence or horseradish peroxidase chemiluminescence using an Amersham ECL Prime Western Blotting Detection Reagent (Fisher Scientific), respectively. For RNA sequencing, RNA was extracted from 16D cells treated with dimethyl sulfoxide or 10 μM enzalutamide for 48 h using a RNeasy Mini Kit (Qiagen; Germantown, MD, USA). Library preparation was performed using the KAPA Stranded mRNA-Seq Kit

(Roche). The workflow consists of mRNA enrichment, cDNA generation, and end repair to generate blunt ends, A-tailing, adaptor ligation, and polymerase chain reaction amplification. Different adaptors were used for multiplexing samples in one lane. The Illumina HiSeq 3000 was used to perform sequencing for 1 × 50 runs. The data have been deposited in NCBI's Gene Expression Omnibus and are accessible through GEO Series accession number GSE202885.

IHC

Tissue sections (3 μm) were subjected to immunohistochemical staining. The sections were stained using anti-TMPRSS2 (clone EPR3861, rabbit, Abcam; 1:16,000), anti-TMPRSS2 (obtained from the Peter Nelson Lab, University of Washington, Seattle, WA, USA; mouse; 1:200), anti-AR (clone SP107, rabbit, Cell Marque, Rocklin, CA, USA; 1:100), anti-AR (441, mouse, Santa Cruz, 1:100), anti-ACE2 (clone MM0073-11A31, mouse, Abcam, 1:200), anti-ACE2 (ab15348, rabbit, Abcam, 1:100), and anti-furin (EPR14674, rabbit, Abcam, 1:600). IHC was carried out on a Dako Link 48 autostainer (Agilent Technologies, Santa Clara, CA, USA), with antibody incubation for 60 min, amplification using Envision FLEX rabbit or mouse linkers, and visualization using the Envision Flex High-sensitivity visualization system (Agilent Technologies).

Nasopharyngeal (NP) swabs

The NP swab specimens obtained from the HITCH subjects were placed in viral transport media and then centrifuged to remove the supernatant fluid. The cell pellets were transferred to a 1.5-mL Eppendorf tube. One drop of warmed HistoGel heated at 42°C was added to each pellet. A clot formed within 3–5 min. The clot was then processed by routine formalin-fixation and paraffin-embedding for histology.

Statistical analysis

Prism v8.3.0 (GraphPad; San Diego, CA, USA) was used to generate graphs and perform statistical analyses. All t-tests conducted were two-sided t-tests with Welch's correction. All error bars represent the standard error of the mean. A *p*-value of <0.01 was considered statistically significant.

Results

Androgen has a minimal effect on TMPRSS2 protein expression in murine or human PCa

Although TMPRSS2 is a canonical AR target in human PCa, it is still unknown whether TMPRSS2 expression is exclusively regulated by androgen in prostate tissue and PCa. To examine the dependency of androgen regulation in TMPRSS2 expression, we assessed the changes in TMPRSS2 protein expression in prostate glands of male mice after ADT. C57BL/6 (n = 9) mice were treated with vehicle or the AR antagonist enzalutamide for 1 week or 2 weeks (*n* = 3 each). Male ICR/scid mice (n = 8) were treated with vehicle (n = 4), enzalutamide or the androgen synthesis inhibitor abiraterone acetate for 10 days (*n* = 2 each). IHC demonstrated no apparent reduction in the TMPRSS2 staining intensity in the prostate glands post enzalutamide or abiraterone treatment compared with the vehicle controls (Fig. 1a–b). The lack of enzalutamide-induced downregulation of TMPRSS2 protein was observed in both young (3 months old) and old (16 months old) C57BL/6 mice (*n* = 9 each). Next, we evaluated the role of androgen in regulating TMPRSS2 expression in human PCa cell lines. Western blot analysis showed no reduction in the TMPRSS2 protein abundance in LNCaP or 16D PCa cells by androgen deprivation or antiandrogen treatment, despite a significant decrease in the mRNA abundance after 48 h of enzalutamide treatment (Fig. 1c–d). Next, we examined the expression of TMPRSS2 in LNCaP xenografts and a hormone sensitive human PCa PDX model after castration or castration + enzalutamide treatment. Immunostaining for TMPRSS2 protein in LNCaP xenografts and the PDX tumors showed no apparent reduction following castration or castration + enzalutamide treatment (Fig. 1e–f). Additionally, TMPRSS2 expression was retained in two cases of AR-negative small cell carcinoma of prostatic origin, indicating AR-independent TMPRSS2 expression in this tumor type (Supplementary Fig. 1a). Together, our results indicate that TMPRSS2 protein expression in benign prostate epithelium and prostatic carcinoma was likely regulated by AR-independent mechanisms, although TMPRSS2 mRNA expression was AR dependent.

TMPRSS2 protein expression is not androgen dependent in murine or human lungs

The effect of androgen on TMPRSS2 expression in murine lungs is controversial, partly due to the lack of validated anti-TMPRSS2 antibodies for IHC in early studies.[7,8] To assess TMPRSS2 protein expression using IHC, we used the Abcam rabbit anti-TMPRSS2 antibody and mouse anti-TMPRSS2 antibody obtained from the Nelson Laboratory at the University of Washington. The review of IHC staining of male human lung tissue showed the presence of AR-positive cells in the bronchial respiratory epithelium and the stroma of alveolar septae. AR positivity was sparse in the alveolar pneumocytes (Supplementary Fig. 2a). TMPRSS2 was diffusely expressed by the bronchial respiratory epithelium, with the staining enriched at the ciliated apical border. ACE2 positivity was rarely detected at the apical border of the bronchial epithelium (Supplementary Fig. 2a–b). TMPRSS2 and ACE2 were expressed by alveolar pneumocytes, with the morphology consistent with type II pneumocytes and macrophages. AR-positive cells in the bronchial epithelium often co-expressed TMPRSS2 and occasionally co-expressed ACE2, while co-expression of AR with TMPRSS2 or ACE2 was rare in alveolar pneumocytes (Supplementary Fig. 2b). In male mice, AR and TMPRSS2 positivity was detected in the alveolar stromal cells, pneumocytes, and rarely in the bronchial epithelium. ACE2 was expressed by both pneumocytes and the bronchial epithelium, with strong staining at the apical border of the bronchial epithelium. Furin was positive in the smooth muscle bundles surrounding the bronchioles, vascular endothelium, and alveolar pneumocytes, and it was weakly positive in the bronchial epithelium (Supplementary Fig. 2c). Next, we tested the effect of an androgen antagonist and androgen deprivation on the expression levels of TMPRSS2, ACE2, and furin in murine lungs. We observed no apparent reduction in TMPRSS2, ACE2, or furin staining in murine lungs following enzalutamide treatment for 1 week or 2 weeks (*n* = 3 each group), regardless of the age of the mouse (Fig. 2a). Similarly, androgen deprivation by surgical castration did not reduce the staining intensity of any of these viral entry proteins in murine lungs (*n* = 6 each) (Supplementary Fig. 3). In agreement with the IHC results in murine studies, immunoblots from three different human lung cancer cell lines showed minimal AR expression as well as a low level of TMPRSS2 expression that was not altered by enzalutamide treatment (Fig. 2b).

Androgen regulates TMPRSS2, ACE2, and furin in murine sinonasal tissue

The infection of SARS-CoV-2 in humans first occurs in the nasal cavity and nasopharynx in the very early phase of COVID-19

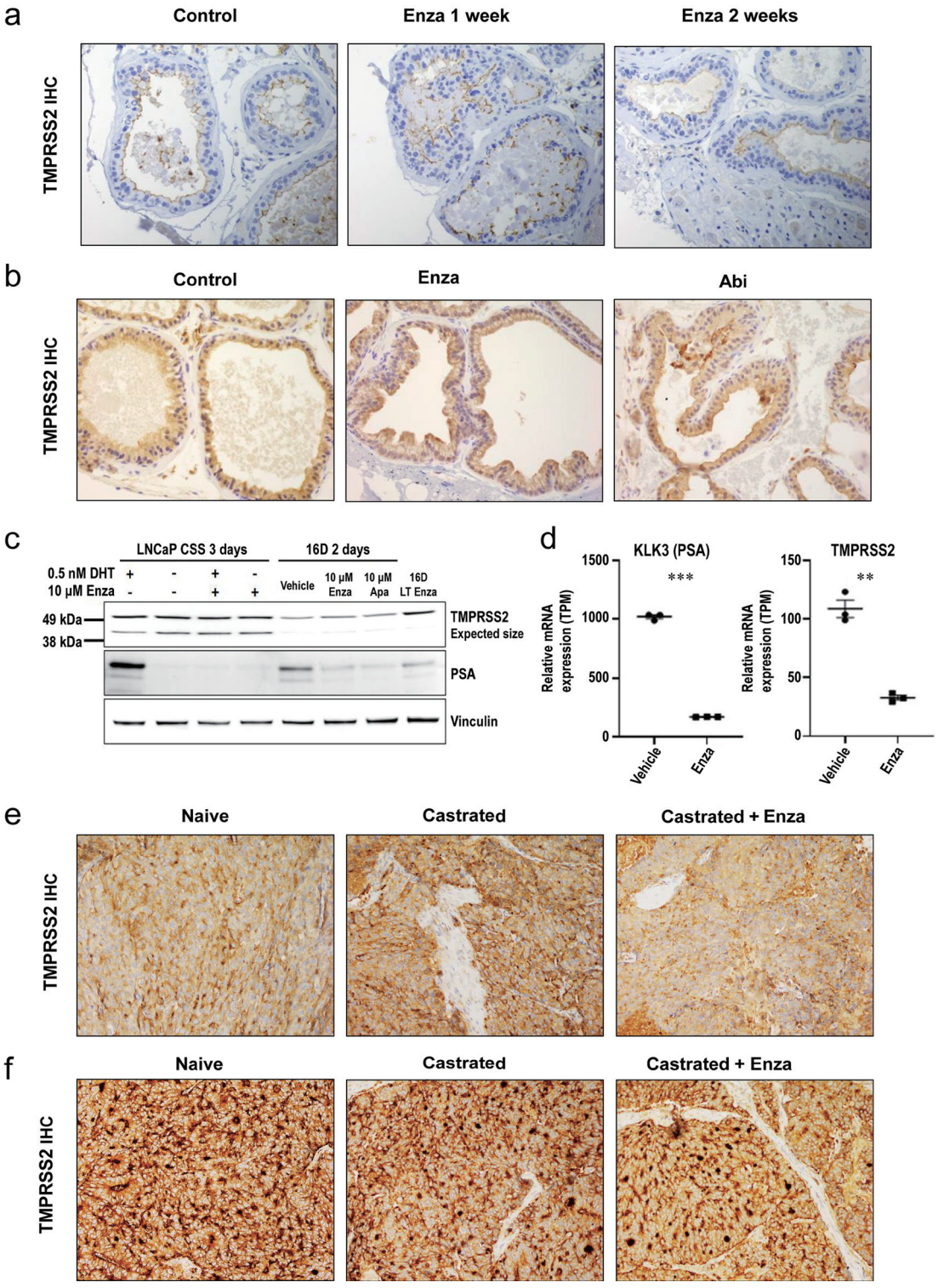

Fig. 1. TMPRSS2 protein expression in the prostate and prostate cancer is not primarily driven by androgen. (a) Representative images of TMPRSS2 IHC of murine prostate glands (n = 18; 9 young and 9 old) treated with vehicle, enzalutamide for 1 week, or enzalutamide for 2 weeks (n = 3 each), respectively. (b) Representative images of TMPRSS2 IHC of murine prostate glands (n = 8) treated with vehicle (n = 4), enzalutamide (n = 2), or abiraterone (n = 2), respectively. (c) Western blots of LNCaP and 16D cells treated with castration, enzalutamide (Enza), or Apalutamide (Apa), demonstrating the expression of TMPRSS2, PSA, and the loading control vinculin. (d) Quantification of RNA sequencing data (TPM) demonstrated reduced mRNA levels of KLK3 (PSA) and TMPRSS2 in 16D cells treated with vehicle or enzalutamide for 48 h. Data represent the unpaired t test with Welch's correction. ***p < 0.001, **p < 0.01. (e, f) Representative images of TMPRSS2 IHC of LNCaP xenografts (e) (n = 2 each) and a patient-derived xenograft (f) at precastration, 7 days post castration, or 7 days post castration + enzalutamide treatment, respectively (n = 2 each). IHC, immunohistochemistry; KLK3, kallikrein 3; PSA, prostate-specific antigen; TMPRSS2, transmembrane serine protease 2.

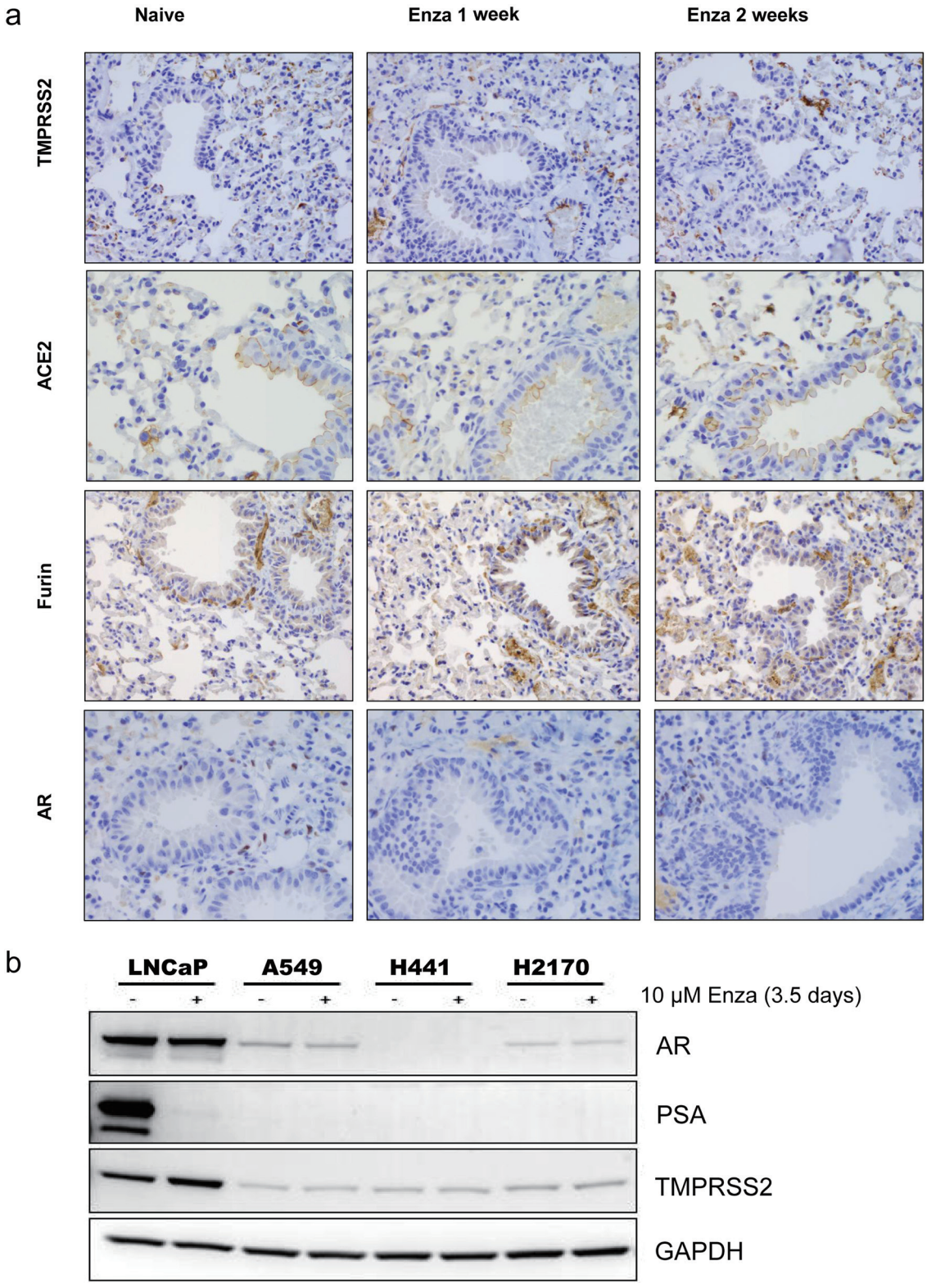

Fig. 2. Androgen signaling showed no effect on regulating the expression of viral entry proteins in murine lungs. (a) Representative images of lungs of mice (9 young and 9 old) treated with vehicle, enzalutamide for 1 week, or enzalutamide for 2 weeks (n = 3 in each group), stained with antibodies against TMPRSS2, ACE2, furin, and AR (all at 200× magnification). (b) Western blots of LNCaP and three different lung cell lines treated with 10 μM enzalutamide for 3.5 days, blotted for AR, PSA, TMPRSS2, and the loading control GAPDH. ACE2, angiotensin-converting enzyme 2; AR, androgen receptor; GAPDH, glyceraldehyde 3-phosphate dehydrogenase; PSA, prostate-specific antigen; TMPRSS2, transmembrane serine protease 2.

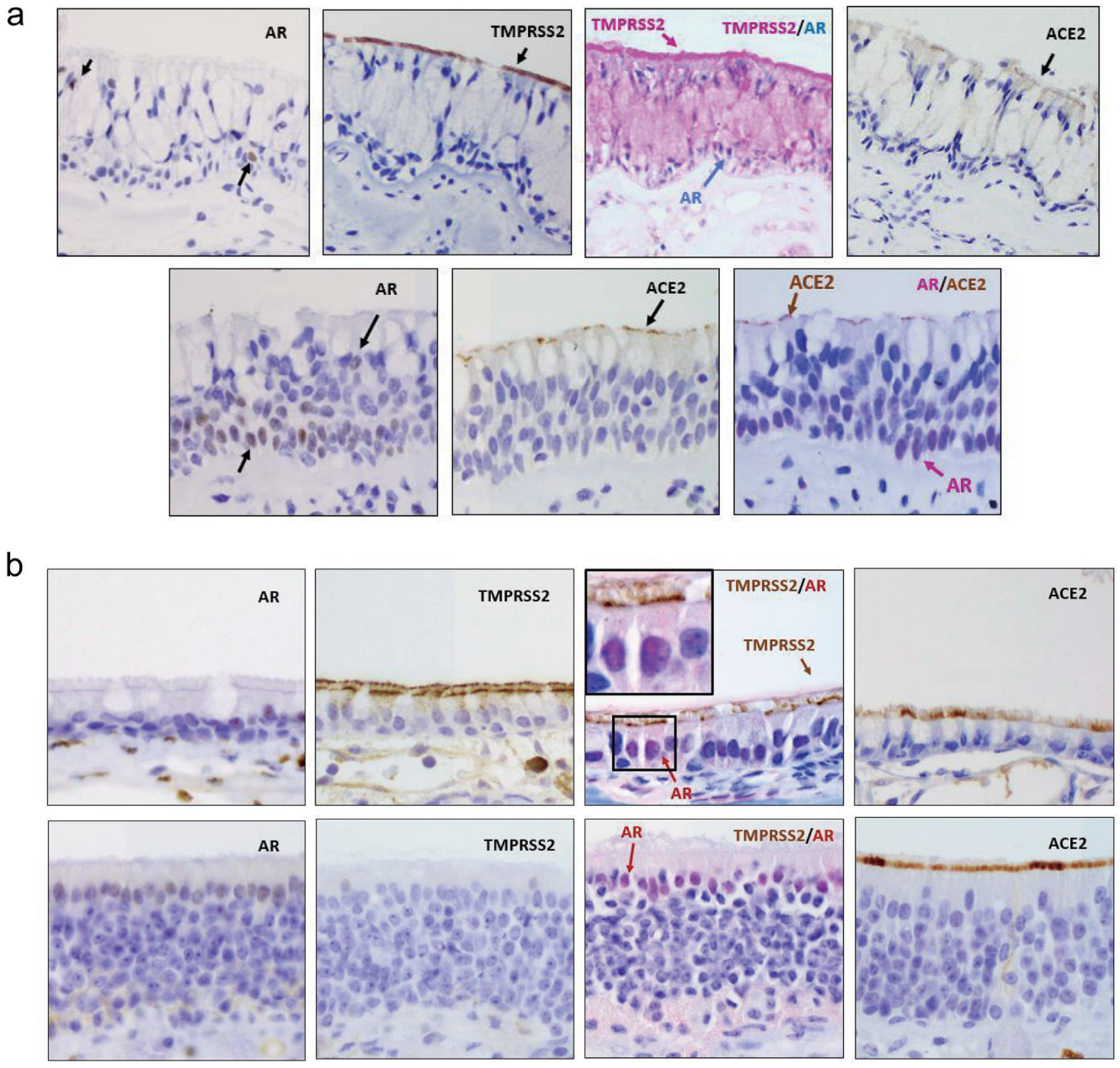

Fig. 3. Co-expression of AR and viral entry proteins in the human and murine sinonasal epithelium. (a) Top panel: Representative images of human middle turbinate stained for AR, TMPRSS2, double-stained for AR (blue) and TMPRSS2 (red), and ACE2; Bottom panel: Representative images of human inferior turbinate stained for AR, ACE2, and double-stained for AR (red) and ACE2 (brown). (b) Representative images of murine sinonasal mucosa stained for AR, TMPRSS2, double-stained for AR (red) and TMPRSS2, and ACE2. Top panel: respiratory epithelium, Bottom panel: olfactory epithelium (all at 400× magnification, except for the inset magnified at 1000× with an oil lens). ACE2, angiotensin-converting enzyme 2; AR, androgen receptor; TMPRSS2, transmembrane serine protease 2.

disease. Subsequently, the virus spreads to the lower respiratory tract, including the bronchi and lungs, the main target organs.[9–11] Accordingly, we sought to assess the potential role of androgen signaling in SARS-CoV-2 entry protein expression in the nasal cavities. First, we performed immunostaining using turbinate specimens from male patients who underwent sinus surgery. The respiratory epithelium showed a low level of AR protein expression. TMPRSS2 and ACE2 colocalized at the ciliated apical border of the respiratory epithelium (Fig. 3a). Co-expression of AR and TMPRSS2 as well as co-expression of AR and ACE2 were easily detected by dual immunostaining. Next, we assessed AR expression in the nasal mucosa of male mice by examining coronal sections of the mouse skull. In the murine nasal cavities, the dorsal portion was lined by the olfactory epithelium, and the ventral portion was lined by the respiratory epithelium. AR was weakly expressed in both the olfactory and respiratory epithelium (Fig. 3b). TMPRSS2, ACE2, and furin were all expressed at the apical border of the respiratory epithelium. TMPRSS2 was expressed in the respiratory epithelium but not in the olfactory epithelium. Co-expression of AR and TMPRSS2 was detected in the respiratory epithelium, as shown in Figure 3b, with the inset showing

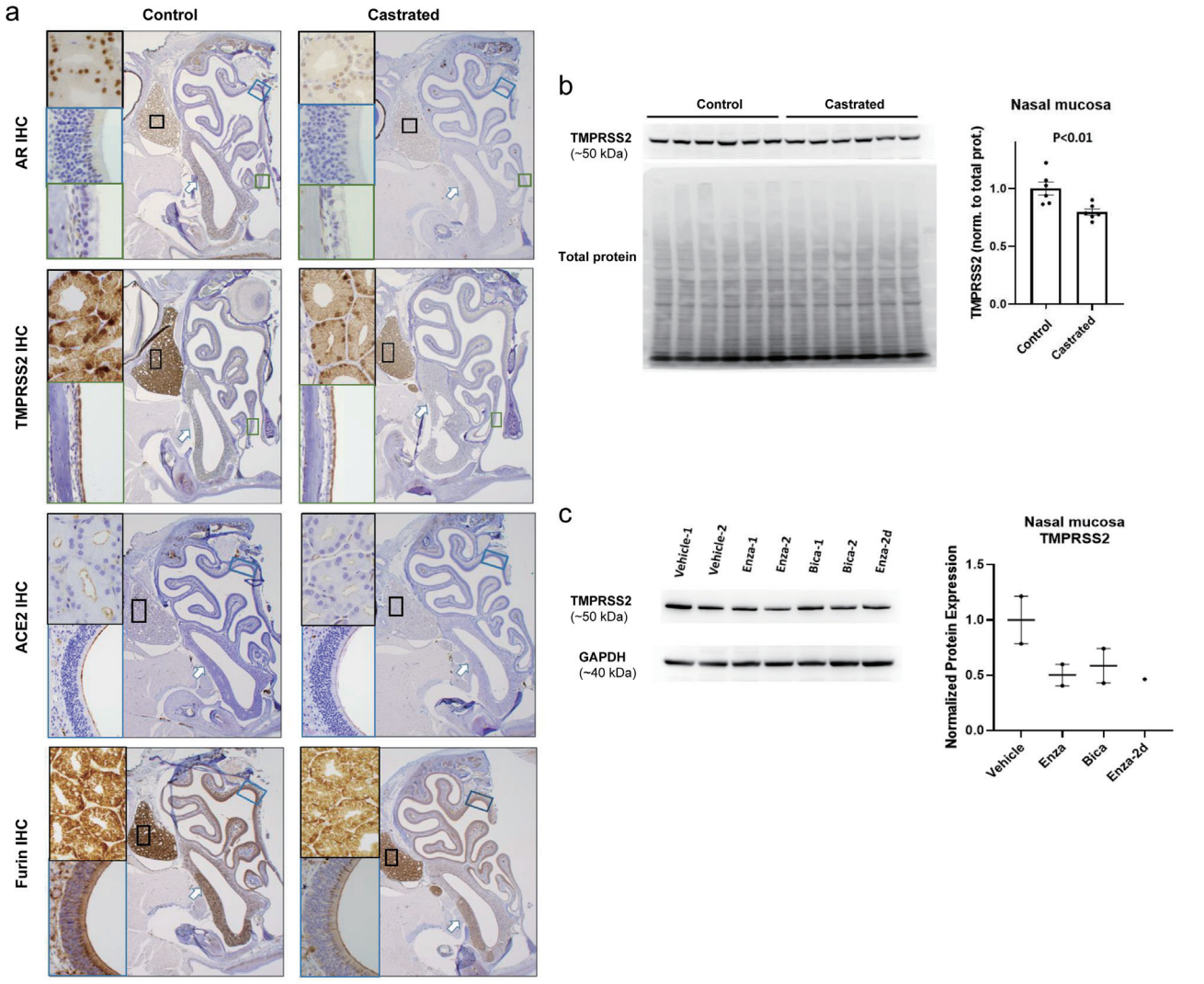

Fig. 4. Castration was associated with reduced TMPRSS2 and ACE2 expression in murine sinonsal tissue and glands. (a) Representative images of coronal sections of mouse skull, control or castrated (n = 6 in each group) at 20× magnification, stained for AR, TMPRSS2, ACE2, and furin (white arrow: minor salivary gland of the maxillary sinus; black box: lacrimal gland; blue box: olfactory epithelium; green box: respiratory epithelium (with insets magnified at 400×). (b) Western blots of the nasal mucosa of control and castrated mice demonstrating the expression of TMPRSS2, with the protein levels normalized by total protein stained with SYPRO RUBY. Quantification of TMPRSS2 staining to the total protein levels shown on the right. (c) Western blots of the nasal mucosa of mice treated with vehicle or antiandrogen for 7 days demonstrating the expression of TMPRSS2 and the loading control GAPDH. Signal quantification is shown on the right. ACE2, angiotensin-converting enzyme 2; AR, androgen receptor; GAPDH, glyceraldehyde 3-phosphate dehydrogenase; TMPRSS2, transmembrane serine protease 2.

colocalization of AR and TMPRSS2 in the same ciliated columnar cells. ACE2 was expressed in both the respiratory and olfactory epithelium, with a stronger expression in the olfactory epithelium (Fig. 3b, 4a). Furin was diffusely expressed in the mucosa of the entire nasal cavity. Interestingly, murine lacrimal glands showed a strong expression of AR, TMPRSS2, ACE2, and furin; whereas the minor salivary glands surrounding the respiratory sinus strongly expressed AR, TMPRSS2, and furin (Fig. 4). Next, we evaluated the effects of ADT on the abundance of these proteins in the sinonasal tissue by treating mice with mock castration or surgical castration (n = 6 in each group). In the castrated mice, the staining intensity of AR, TMPRSS2, ACE2, and furin was markedly reduced in the lacrimal glands, and it was mildly reduced in the nasal epithelium and minor salivary glands compared with that of the control mice (Fig. 4a). Immunoblots of mouse nasal mucosa from the same set of mice demonstrated a mild reduction of TMPRSS2 expression in the castrated mice (Fig. 4b). Additionally, we treated mice with the androgen antagonist enzalutamide or bicalutamide (n= 3 each) for 1 week. AR blockade was associated with a mild reduction of TMPRSS2, ACE2, and furin expression in the mouse nasal mucosa, as detected by western blot and IHC (Fig. 4c, Fig. 4). Table 1 summarizes all experiments that were conducted in this study to assess the role of androgen in modulating the expression of viral entry proteins.

Sample inadequacy prohibited IHC evaluation for NP epithelium collected from HITCH patients

Next, we sought to examine the potential antiviral effect of ADT in male COVID-19 patients. First, we established the

Table 1. Summary of results by tissue type and treatment modality

Tissue/Cell Type	Treatment	Reduced Expression Detected by IHC (or WB)			
		TMPRSS2	ACE2	Furin	AR
Mouse					
Prostate	Enzalutamide or abiraterone	No			
Lungs	Castration or enzalutamide	No	No	No	No
Sinonasal mucosa	Castration or enzalutamide	Yes (IHC&WB)	Yes	Yes	Yes
Lacrimal glands	Castration or enzalutamide	Yes	Yes	Yes	Yes
Minor salivary glands of sinus	Castration or enzalutamide	Yes	No	Yes	Yes
Human					
Prostate					
Prostate cancer cell lines					
LNCaP	Castration ± enzalutamide	No (WB)			
16D	Enzalutamide or apalutamide	No (WB)			
HSPC xenografts					
LNCaP xenograft	Castration ± enzalutamide	No			
Patient PDX	Castration ± enzalutamide	No			
Lung					
Lung cancer cell lines					
A549	Enzalutamide	No (WB)			No (WB)
H441	Enzalutamide	No (WB)			No (WB)
H2170	Enzalutamide	No (WB)			No (WB)

IHC, Immunohistochemistry; WB, Western Blot; HSPC, Hormone sensitive prostate cancer.

protocol of NP cell block preparation and subsequent IHC staining using NP swabs obtained from healthy male donors (Supplementary Fig. 5a). The NP swab generated abundant respiratory epithelial cells, with most cells strongly positive for TMPRSS2 and a small subset of cells weakly positive for AR and ACE2. Subsequently, we collected paired NP swabs from HITCH trial patients at hospital day 1 (just prior to medical castration) and day 8 (one week after medical castration). Unexpectedly, most of the NP samples obtained from the HITCH patients generated few epithelial cells; therefore, there were insufficient cells for IHC evaluation. In rare NP samples with good cellularity, we were able to detect the co-expression of viral guide RNA and TMPRSS2 in ciliated epithelial cells (Supplementary Fig. 5b). Paired day 1/day 8 samples from two trial patients showed no apparent changes in the TMPRSS2 staining intensity in rare NP cells (Supplementary Fig. 5c). Further optimization of the methodology was not able to increase the cellularity of the patient samples. Thus, we discontinued NP swab collection, given the risk of disease contraction during the sample collection and handling.

Discussion

Randomized clinical trials have failed to show that ADT improves the clinical outcomes of hospitalized male COVID-19 patients.[4,5,12] Murine studies have reported conflicting data on androgen-mediated regulation of the expression of viral entry proteins in the lungs.[6–8,13,14] In our IHC survey of mouse and human tissues, we detected the co-expression of AR and viral entry proteins in sinonasal tissues and the bronchial epithelium, while the co-expression was rarely detected in the pulmonary alveolar tissue. In the mouse studies, castration and AR antagonist treatment were associated with the reduced expression of viral entry proteins in the sinonasal tissue but failed to do so in the lungs.

Our observations in the murine experiments do not align with prior studies that demonstrated androgen-mediated TMPRSS2 and ACE2 expression in the lungs.[6,7] The discrepancy is likely due to the difference in detection methods. Qiao *et al*.[5] measured TMPRSS2 expression using RNA sequencing and RNA *in-situ* hybridization. The authors did not measure TMPRSS2 protein expression in murine or human lungs due to the lack of a suitable IHC antibody. Likewise, they showed co-expression of AR and viral RNA in murine and human lungs using *in-situ* hybridization dual staining. Importantly, the transcript and protein levels of many genes are poorly correlated, including for AR-regulated genes. In support of this notion, enzalutamide reduced TMPRSS2 mRNA expression but did not reduce the TMPRSS2 protein levels in PCa cell lines (Fig. 1c–d). In our dual IHC staining experiments, the co-expression of AR and ACE2 was rare in the human alveolar epithelium (Supplementary Fig. 2b). In line with our findings, Baratchian *et al*. found that treatment with enzalutamide did not decrease pulmonary TMPRSS2 or ACE2 protein expression in male mice.[13] Similarly, Li *et al*. have reported that enzalutamide treatment failed to downregulate TMPRSS2 expression in mouse lungs and human lung organoids. Moreover, they observed that enzalutamide treatment did not inhibit SARS-CoV-2-driven entry into lung cells in mouse models.[8] Similarly, a recent study has shown that enzalutamide treatment did not suppress TMPRSS2 mRNA expression and had no impact on SARS-CoV-2 infection in differentiated human bronchial epithelial cells.[14]

In our study, the co-expression of AR with TMPRSS2 or ACE2 was detected in human and murine sinonasal mucosa (Fig. 3–4). Castration or AR antagonist treatment down-regulated the expression of TMPRSS2, ACE2, and furin in murine sinonasal tissue. Notably, the AR expression in the lacrimal glands and minor salivary glands of the sinus was much stronger compared with that in the sinonasal epithelium, indicating that those adjacent exocrine glands are more sensitive to ADT. While the nasal epithelium is a putative primary target for SARS-CoV-2 replication in the early stage of COVID-19,[9–11,15] recent studies have shown that the salivary glands and lacrimal glands are potential primary targets in early COVID-19.[16–20] The lacrimal glands and ducts may serve as a part of the ocular route of viral infection.[16,21] The salivary glands are potential viral reservoirs for COVID-19 asymptomatic infection.[19,22,23] Based on these findings, we speculate that ADT is potentially effective in men with early COVID-19, when the virus infects and replicates in the sinonasal tissue and adjacent organs. Nevertheless, our study has several limitations that must be addressed. We did not perform a SARS-CoV-2 viral infection experiment in mice, which would require transduction of humanized ACE2. Further, such experiments would require Biosafety Level 3 laboratories, which was not feasible during the execution of our study. In addition, we were not able to obtain evidence of AR-mediated TMPRSS2 expression in human NP mucosa due to inadequate NP swab samples obtained from patients in the HITCH study.

The findings from our study implied a role of ADT in the early NP stage of COVID-19 but not in the pneumonia stage. This observation partially explains the failure of ADT in hospitalized men with COVID-19 in clinical trials, including the HITCH trial. The negative results of ADT in hospitalized patients may be traced to multiple factors. For instance, the HITCH trial reported reduced serum testosterone levels in the placebo group at day 8 and day 15, leading to a smaller difference in the serum testosterone levels between the degarelix group and the placebo group.[4] Men with critical illness frequently have decreased serum testosterone levels, through a decrease in adrenal and gonadal androgen synthesis.[24–26] This observation further argues against the utility of ADT in late COVID-19. As such, there may be a limited window for ADT to be beneficial, i.e., when the viral infection mainly involves the nasopharynx and when the patients have normal testosterone levels. To test the benefit of ADT in early COVID-19, Cadegiani *et al*. treated male COVID-19 outpatients with a short course of androgen blockade (ClinicalTrials.gov Identifier: NCT04446429; EAT-DUTA AndroCoV trial in Brazil).[27–29] However, the benefit of ADT in early COVID-19 remains inconclusive, and we are awaiting results from independent trials.

Conclusions

We detected androgen-dependent regulation of TMPRSS2 and ACE2 in mouse sinonasal tissue but not in the mouse lungs. Our findings indicate a potential protective role of ADT in men with early-stage COVID-19.

Acknowledgments

The authors would like to thank Drs. Peter S. Nelson, Lawrence D. True, and Colm M. Morrissey at the University of Washington & Fred Hutchinson Cancer Research Center for providing the anti-TMPRSS2 antibody. The authors would like to thank Clara Magyar and Dr. Samuel French for the tissue support from the Translational Pathology Core Laboratory at UCLA. Parts of this study have been presented and published as an abstract at the United States and Canadian Academy of Pathology Annual Meeting in 2021.

Funding

The authors gratefully acknowledge research support from the UCLA David Geffen School of Medicine – Broad Stem Cell Research Center (BSCRC) COVID-19 Research Award for this project. HY received research support from the Prostate Cancer Foundation, Dana-Farber/Harvard Cancer Center Prostate Specialized Program of Research Excellence (SPORE) National Cancer Institute (NCI) P50, and the UCLA Prostate SPORE NCI P50 CA092131. SPB received support from NCI P01 CA163227. ASG is supported by the NCI R01CA237191, American Cancer Society award RSG-17-068-01-TBG, and the UCLA Prostate SPORE NCI P50 CA092131.

Conflict of interest

The authors have no conflicts of interest related to this publication.

Author contributions

Study design, performance of experiments, analysis and interpretation of data, critical revision (RRH); performance of experiments, analysis and interpretation of data, statistical analysis (JMG, TH); study design, analysis and interpretation of data, critical funding, administration, technical and material support (LYZ); performance of experiments (WBY); technical support, administration (JYR); performance of experiments, analysis and interpretation of data (JWR); technical and material support (SPB); technical and material support, administration (NGN); study design, analysis and interpretation of data, critical revision, administration, material support (MBR); Study design, analysis and interpretation of data, technical and material support (AG); study design, analysis and interpretation of data, manuscript writing, critical revision, administration, technical and material support (HY). All authors have made a significant contribution to this study and have approved the final manuscript.

Ethical statement

This study was carried out in accordance with the recommendations in the Guide for the Care and Use of Laboratory Animals of the National Institutes of Health. The protocol was approved by the Animal Research Committee on the Ethics of Animal Experiments of the University of California at Los Angeles (Protocol Number: ARC-2017-020). All surgeries were performed under sodium pentobarbital anesthesia, and all efforts were made to minimize suffering.

Data sharing statement

Additional data (figures) are included within the supplementary materials accompanying this publication.

References

[1] Chakravarty D, Nair SS, Hammouda N, Ratnani P, Gharib Y, Wagaskar V, *et al*. Sex differences in SARS-CoV-2 infection rates and the potential link to prostate cancer. Commun Biol 2020;3(1):374. doi:10.1038/s42003-020-1088-9, PMID:32641750.

[2] Bestle D, Heindl MR, Limburg H, Van Lam van T, Pilgram O, Moulton H, *et al*. TMPRSS2 and furin are both essential for proteolytic activation of SARS-CoV-2 in human airway cells. Life Sci Alliance 2020;3(9):e202000786. doi:10.26508/lsa.202000786, PMID:32703818.

[3] Montopoli M, Zumerle S, Vettor R, Rugge M, Zorzi M, Catapano CV, *et al*.

Androgen-deprivation therapies for prostate cancer and risk of infection by SARS-CoV-2: a population-based study (N = 4532). Ann Oncol 2020; 31(8):1040–1045. doi:10.1016/j.annonc.2020.04.479, PMID:32387456.
[4] Nickols NG, Mi Z, DeMatt E, Biswas K, Clise CE, Huggins JT, *et al*. Effect of Androgen Suppression on Clinical Outcomes in Hospitalized Men With COVID-19: The HITCH Randomized Clinical Trial. JAMA Netw Open 2022;5(4):e227852. doi:10.1001/jamanetworkopen.2022.7852, PMID:35438754.
[5] Welén K, Rosendal E, Gisslén M, Lenman A, Freyhult E, Fonseca-Rodríguez O, *et al*. A Phase 2 Trial of the Effect of Antiandrogen Therapy on COVID-19 Outcome: No Evidence of Benefit, Supported by Epidemiology and In Vitro Data. Eur Urol 2022;81(3):285–293. doi:10.1016/j.eururo.2021.12.013, PMID:34980495.
[6] Deng Q, Rasool RU, Russell RM, Natesan R, Asangani IA. Targeting androgen regulation of TMPRSS2 and ACE2 as a therapeutic strategy to combat COVID-19. iScience 2021;24(3):102254. doi:10.1016/j.isci.2021.102254, PMID:33681723.
[7] Qiao Y, Wang XM, Mannan R, Pitchiaya S, Zhang Y, Wotring JW, *et al*. Targeting transcriptional regulation of SARS-CoV-2 entry factors ACE2 and TMPRSS2. Proc Natl Acad Sci U S A 2021;118(1):e2021450118. doi:10.1073/pnas.2021450118, PMID:33310900.
[8] Li F, Han M, Dai P, Xu W, He J, Tao X, *et al*. Distinct mechanisms for TMPRSS2 expression explain organ-specific inhibition of SARS-CoV-2 infection by enzalutamide. Nat Commun 2021;12(1):866. doi:10.1038/s41467-021-21171-x, PMID:33558541.
[9] Sungnak W, Huang N, Bécavin C, Berg M, Queen R, Litvinukova M, *et al*. SARS-CoV-2 entry factors are highly expressed in nasal epithelial cells together with innate immune genes. Nat Med 2020;26(5):681–687. doi:10.1038/s41591-020-0868-6, PMID:32327758.
[10] Cevik M, Kuppalli K, Kindrachuk J, Peiris M. Virology, transmission, and pathogenesis of SARS-CoV-2. BMJ 2020;371:m3862. doi:10.1136/bmj.m3862, PMID:33097561.
[11] Martines RB, Ritter JM, Matkovic E, Gary J, Bollweg BC, Bullock H, *et al*. Pathology and Pathogenesis of SARS-CoV-2 Associated with Fatal Coronavirus Disease, United States. Emerg Infect Dis 2020;26(9):2005–2015. doi:10.3201/eid2609.202095, PMID:32437316.
[12] Cadegiani FA, Zimerman RA, Fonseca DN, Correia MN, Muller MP, Bet DL, *et al*. Final Results of a Randomized, Placebo-Controlled, Two-Arm, Parallel Clinical Trial of Proxalutamide for Hospitalized COVID-19 Patients: A Multiregional, Joint Analysis of the Proxa-Rescue AndroCoV Trial. Cureus 2021;13(12):e20691. doi:10.7759/cureus.20691, PMID:34976549.
[13] Baratchian M, McManus JM, Berk MP, Nakamura F, Mukhopadhyay S, Xu W, *et al*. Androgen regulation of pulmonary AR, TMPRSS2 and ACE2 with implications for sex-discordant COVID-19 outcomes. Sci Rep 2021;11(1):11130. doi:10.1038/s41598-021-90491-1, PMID:34045511.
[14] Guo W, Porter LM, Crozier TW, Coates M, Jha A, McKie M, *et al*. Topical TMPRSS2 inhibition prevents SARS-CoV-2 infection in differentiated human airway cultures. Life Sci Alliance 2022;5(4):e202101116. doi:10.26508/lsa.202101116, PMID:35110354.
[15] Ahn JH, Kim J, Hong SP, Choi SY, Yang MJ, Ju YS, *et al*. Nasal ciliated cells are primary targets for SARS-CoV-2 replication in the early stage of COVID-19. J Clin Invest 2021;131(13):148517. doi:10.1172/JCI148517, PMID:34003804.
[16] Baig AM, Ahmad S, Khaleeq A, Rafique H, Rajput S, Angez M, *et al*. Ocular COVID-19: Eyes as a Reservoir to Conceal and Spread SARSCoV- 2. Infect Disord Drug Targets 2021;21(4):480–483. doi:10.2174/1871526520999200729182242, PMID:32729433.
[17] Martin G, Wolf J, Lapp T, Agostini HT, Schlunck G, Auw-Hädrich C, *et al*. Viral S protein histochemistry reveals few potential SARS-CoV-2 entry sites in human ocular tissues. Sci Rep 2021;11(1):19140. doi:10.1038/s41598-021-98709-y, PMID:34580409.
[18] Matuck BF, Dolhnikoff M, Duarte-Neto AN, Maia G, Gomes SC, Sendyk DI, *et al*. Salivary glands are a target for SARS-CoV-2: a source for saliva contamination. J Pathol 2021;254(3):239–243. doi:10.1002/path.5679, PMID:33834497.
[19] Xu J, Li Y, Gan F, Du Y, Yao Y. Salivary Glands: Potential Reservoirs for COVID-19 Asymptomatic Infection. J Dent Res 2020;99(8):989. doi:10.1177/0022034520918518, PMID:32271653.
[20] Iwasaki S, Fujisawa S, Nakakubo S, Kamada K, Yamashita Y, Fukumoto T, *et al*. Comparison of SARS-CoV-2 detection in nasopharyngeal swab and saliva. J Infect 2020;81(2):e145–e147. doi:10.1016/j.jinf.2020.05.071, PMID:32504740.
[21] Ho D, Low R, Tong L, Gupta V, Veeraraghavan A, Agrawal R. COVID-19 and the Ocular Surface: A Review of Transmission and Manifestations. Ocul Immunol Inflamm 2020;28(5):726–734. doi:10.1080/09273948.2020.1772313, PMID:32543262.
[22] Pascolo L, Zupin L, Melato M, Tricarico PM, Crovella S. TMPRSS2 and ACE2 Coexpression in SARS-CoV-2 Salivary Glands Infection. J Dent Res 2020; 99(10):1120–1121. doi:10.1177/0022034520933589, PMID:32479133.
[23] Tanaka J, Senpuku H, Ogawa M, Yasuhara R, Ohnuma S, Takamatsu K, *et al*. Human induced pluripotent stem cell-derived salivary gland organoids model SARS-CoV-2 infection and replication. Nat Cell Biol 2022;24(11):1595–1605. doi:10.1038/s41556-022-01007-6, PMID:36253535.
[24] Foster MA, Taylor AE, Hill NE, Bentley C, Bishop J, Gilligan LC, *et al*. Mapping the Steroid Response to Major Trauma From Injury to Recovery: A Prospective Cohort Study. J Clin Endocrinol Metab 2020;105(3):925–937. doi:10.1210/clinem/dgz302, PMID:32101296.
[25] Wasyluk W, Wasyluk M, Zwolak A. Sepsis as a Pan-Endocrine Illness-Endocrine Disorders in Septic Patients. J Clin Med 2021;10(10):2075. doi:10.3390/jcm10102075, PMID:34066289.
[26] Dong Q, Hawker F, McWilliam D, Bangah M, Burger H, Handelsman DJ. Circulating immunoreactive inhibin and testosterone levels in men with critical illness. Clin Endocrinol (Oxf) 1992;36(4):399–404. doi:10.1111/j.1365-2265.1992.tb01466.x, PMID:1424172.
[27] Cadegiani FA, McCoy J, Gustavo Wambier C, Vaño-Galván S, Shapiro J, Tosti A, *et al*. Proxalutamide Significantly Accelerates Viral Clearance and Reduces Time to Clinical Remission in Patients with Mild to Moderate COVID-19: Results from a Randomized, Double-Blinded, Placebo-Controlled Trial. Cureus 2021;13(2):e13492. doi:10.7759/cureus.13492, PMID:33633920.
[28] McCoy J, Goren A, Cadegiani FA, Vaño-Galván S, Kovacevic M, Situm M, *et al*. Proxalutamide Reduces the Rate of Hospitalization for COVID-19 Male Outpatients: A Randomized Double-Blinded Placebo-Controlled Trial. Front Med (Lausanne) 2021;8:668698. doi:10.3389/fmed.2021.668698, PMID:34350193.
[29] Cadegiani FA, McCoy J, Gustavo Wambier C, Goren A. Early Antiandrogen Therapy With Dutasteride Reduces Viral Shedding, Inflammatory Responses, and Time-to-Remission in Males With COVID-19: A Randomized, Double-Blind, Placebo-Controlled Interventional Trial (EAT-DUTA AndroCoV Trial - Biochemical). Cureus 2021;13(2):e13047. doi:10.7759/cureus.13047, PMID:33643746.